AIAA JOURNAL
Vol. 42, No. 3, March 2004

Prediction of Mean Droplet Size of Sprays Issued from Wall Impingement Injector

Takao Inamura* and Hideki Yanaoka†
Hirosaki University, Hirosaki 036-8561, Japan
and
Terutoshi Tomoda‡
Toyota Motor Corporation, Susono 410-1193, Japan

The purpose of this study is to make a numerical model that predicts the spray characteristics of a wall impingement injector. The film flow on the wall was analyzed theoretically using the laminar boundary-layer model. The biquadratic velocity profile was employed for the laminar boundary layer. The thickness of the liquid film on the wall was measured by an automatic thickness measurement system, which was newly developed for the present study and is based on the contact needle method. From the measurements, the film thickness decreased first toward the periphery, and then increased along the line that was perpendicular to the liquid injection direction. The theoretical analysis of the film thickness on the wall agreed well with the measurements. The sizes of the droplets from the newly developed wall impingement injector were predicted by using the proposed theoretical analysis of a film flow and the existing liquid-film breakup model. From the measurements from the phase Doppler particle analyzer, the mean droplet size decreased once toward the spray periphery and then increased. This trend of the droplet size was coincident to that of the liquid-film thickness at the edge of the wall. The mean droplet size decreased as the liquid injection pressure increased. The predictions of the droplet size agreed well with the measurements.

Nomenclature

A = constant defined by Eq. (10)
a = radius of impinging liquid jet
B = constant defined by Eq. (11)
D = diameter of liquid injection nozzle
d_L = liquid stem diameter
d_m = mean droplet diameter defined by Eq. (16)
d_{32} = Sauter mean diameter
h = liquid-film thickness
K = constant defined by Eq. (18)
L = distance from stagnation point to solid wall edge
Oh = Ohnesorge number
P_i = liquid injection pressure
Q = liquid volume flow rate, $= \pi a^2 U_0$
Re = Reynolds number defined by Eq. (8)
r = radial distance from stagnation point
$r_{\phi 0}$ = radial distance in ϕ direction from stagnation point to point where laminar boundary layer reaches to liquid film surface
U = velocity of liquid-film surface
U_e = mean velocity of liquid film at solid wall edge
U_m = mean velocity of liquid film
U_0 = impingement velocity of liquid jet
u = velocity of liquid in radial direction
w = space between jet center line and streamline passing stagnation point defined by Eq. (3)
X = coordinate perpendicular to center line of spray in spray sheet (illustrated in Fig. 3)
x = coordinate perpendicular to center line of liquid-film flow on solid wall surface (illustrated in Fig. 7)
y = coordinate along centerline of liquid-film flow on solid wall surface from impingement point (illustrated in Fig. 7)
Z = coordinate in vertical direction (illustrated in Fig. 3)
z = coordinate perpendicular to solid wall
α = coordinate in azimuthal direction in cross section of liquid jet
δ = boundary-layer thickness
η = nondimensional coordinate
θ = impingement angle
μ = viscosity
ν = kinetic viscosity
ρ = density
σ = surface tension
ϕ = coordinate in azimuthal direction on solid wall

Subscripts

a = surrounding air
e = wall edge
l = liquid
ϕ = ϕ direction

Superscript

$*$ = nondimensional value

Introduction

THE liquid-film atomization type of injector has an advantage of an efficient atomization compared to the liquid-column atomization type. This is because the contact area between liquid and air at the atomization stage of the film atomization type is much larger than that of the column atomization type. Thus, the prefilming type of injector has been adopted in many engines, such as automobile, gas turbine, and liquid-fueled rocket engines. To generate the liquid film, the following methods are considered: by centrifugal force, by injection from a narrow gap, by impingement between liquid jets, and by impingement of a liquid jet onto a solid wall. The method of impingement of a liquid jet onto a solid wall has advantages, such

Received 25 July 2002; revision received 9 September 2003; accepted for publication 9 September 2003.

*Professor, Faculty of Science and Technology, 3 Bunkyo-cho. Senior Member AIAA.
†Associate Professor, Faculty of Science and Technology. 3 Bunkyo-cho.
‡Group Manager, Power Train Engineering Div. 2, 1200 Mishuku.

as low injection pressure loss and high controllability of a generated liquid film. In a previous paper, the wall impingement injector was newly developed.[1] The high-speed liquid jet impinges obliquely onto the solid wall, and the thin liquid film is generated on the wall. The thin liquid film disintegrates into droplets after it leaves the wall edge, and the flat spray sheet is generated.

On the other hand, the numerical simulation of the spray flow has become beneficial for engine design and for obtaining a better understanding of the combustion process.[2,3] The major problem of the numerical simulation of the spray flow is that the practical direct simulation of the liquid atomization process is impossible at the present state. Therefore, the best way to simulate the spray flow is to employ the precise model of the liquid disintegration. Thus, the semi-empirical model of the liquid disintegration mechanism has become very important in predicting the spray characteristics.[4–7]

The instability of the liquid film was investigated theoretically by York et al.,[8] Squire,[9] Hagerty and Shea,[10] and Dombrowski and Johns.[11] They deduced the growth rate equation of a wave on the liquid surface as a function of the wave number, film velocity, and the physical properties of the liquid and surrounding gas. Hagerty and Shear indicated that the growth rate of a sinuous wave is greater than that of a dilational wave for all wave numbers in an unstable wave regime.

The disintegration mechanism of the liquid film was investigated theoretically by Fraser et al.[12] They employed the hypothesis that the liquid film disintegrates into the liquid stem every half-wavelength of a sinuous wave, then the liquid stem disintegrates into droplets every one wavelength. Miyamoto et al. predicted the droplet size of the spray numerically generated by the disintegration of the liquid film issued from the internal mixing airblast atomizer.[13] They obtained the liquid-film thickness by analyzing the two-phase flow in the atomizer. Han et al. predicted the droplet size of the spray issued from a swirl atomizer by applying the blob model.[14] Nagaoka and Kawamura analyzed the spray behavior issued from the fuel injector of a direct-injection spark-ignition gasoline engine.[15] He used the theoretical analysis of Dombrowski and Johns,[11] Dombrowski et al.,[16] and Dombrowski and Hooper.[17] to estimate the droplet size.

In this paper, the liquid-film flow on the solid wall was analyzed theoretically, and the mean droplet size of the spray issued from the newly developed wall impingement injector that had employed the disintegration model of the liquid film proposed by Fraser et al. was predicted.[12] The thicknesses of the liquid film flowing over the solid wall were measured by the newly developed automatic film thickness measurement system. The droplet sizes measured by the phase Doppler particle analyzer (PDPA) system in the previous paper[1] were used for comparison with the calculations. The predicted film thickness and the mean droplet size were compared with the measurements.

Experimental Apparatus

The rough sketch of the experimental apparatus is shown in Fig. 1. A liquid jet injected from the hole injector impinges onto a brass plate. The impingement angle can be set to a desired value by the mechanical stage. In the present study, the two types of injectors were prepared as shown in Figs. 2a and 2b. Nozzle 1 was designed so that the velocity distribution of the liquid flow at the exit can develop fully. This nozzle was used to verify the accuracy of the film thickness measurement system. nozzle 2 was designed especially in accordance to the design guide of a water jet so that no turbulence nor cavitation can be generated in the liquid flow and prevent the liquid jet issued from the injector hole from spreading. The details of the experimental apparatus were explained in a previous paper.[1]

The spray characteristics were measured by the PDPA with a 300-mW Ar^+ laser (Aerometric Co.) in a previous paper.[1] The validation rate of the droplet size measurement was around 80% throughout the measurements. The injector tip and the coordinate system used in the spray characteristics measurement are shown in Figs. 2c and 3. The liquid injection nozzle is the same as nozzle 2 shown in Fig. 2b. The impingement angle is 30 deg, and the distance from the impingement point to the solid wall edge is 3 mm. The injector was mounted on the mechanical stage so that the distance between the

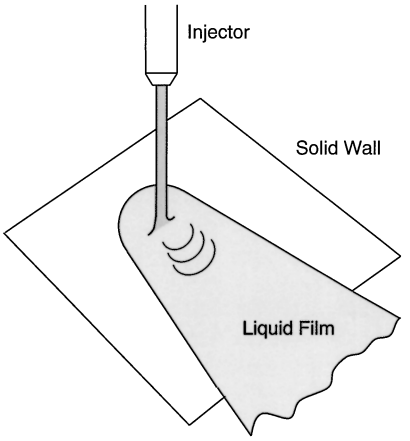

Fig. 1 Concept of experimental apparatus.

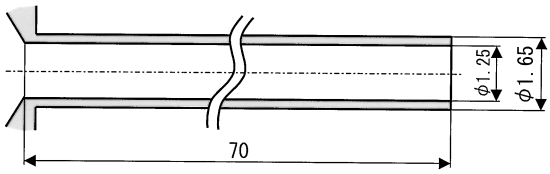

a) Nozzle 1

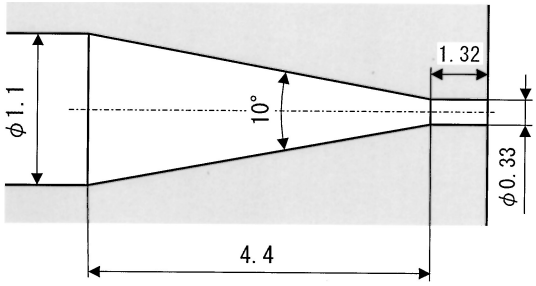

b) Nozzle 2

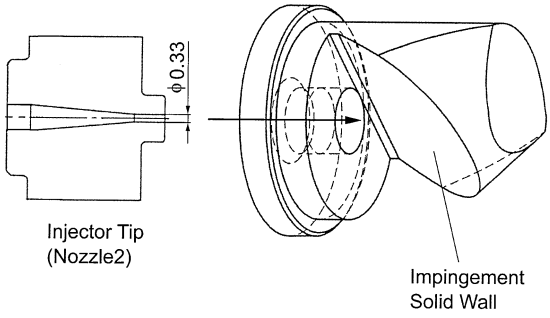

c) Injector

Fig. 2 Liquid injection nozzles.

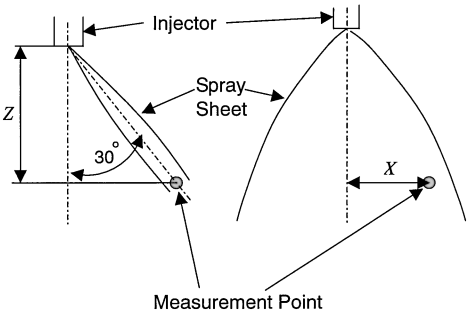

Fig. 3 Coordinate system employed in spray characteristics measurement.

injector and the measurement point of the spray droplet size can be set up precisely. The vertical distance Z between the injector and the measurement point is fixed at 50 mm. The droplet size varies spatially in the direction of film thickness. Therefore, the droplet size measurements were carried out at the center of the spray plume in the direction of film thickness.

The contact needle method was used to measure the thickness of the film flowing over the solid wall. The principle of the film thickness measurement is illustrated in Fig. 4. An electric voltage of 15 V is applied between the needle probe and the liquid film. When the probe touches the film, the electric circuit is closed, and the voltage difference across the resistance is produced. The voltage difference was measured by a voltmeter. Because the liquid-film surface fluctuates, the signal detected by the voltmeter also fluctuates. In the present study, the position of the needle probe tip, where the ratio of the total closed circuit time to the total measurement time is 50%, was regarded as the position of the film surface. The newly developed film thickness measurement system is illustrated in Fig. 5. This system consists of three parts, that is, the controller of an injector, the controller of a stepping motor, and the electric circuit that detects the contact of the needle probe to the liquid-film surface. These parts are controlled by the computer.

Figure 6 shows the flowchart of the film thickness measurement. The measurement starts 30 ms after the valve open signal is sent to the injector. This occurs in order to prevent measuring the thick rim at the tip of the liquid film. The system checks whether the needle probe has made contact with the liquid; if not, the stepping motor proceeds one step (3.2 μm) every time. As soon as the needle probe makes contact with the liquid, the stepping motor stops, and the film thickness is calculated automatically from the position of a needle probe tip. The film thickness measurement of one measurement point is completed in less than 300 ms.

Because the perfect in situ measurement system of a liquid-film thickness does not exist now, it is difficult to show the accuracy of the present measurement system of liquid-film thickness. The accuracy also changes according to the condition of a liquid-film surface. In the case of normal impingement and low jet Reynolds number, the present theoretical analysis seems to be able to predict the film thickness with considerable accuracy.[18] From the comparison of the film thickness between the measurement and the theoretical analysis in the case of normal impingement and low jet Reynolds number, the accuracy of the present measurement system of liquid-film thickness is roughly estimated to be less than 20 μm.

The physical properties of the used liquids are shown in Table 1. Tap water was used in the film thickness measurement as the injection liquid because it was necessary that the liquid have

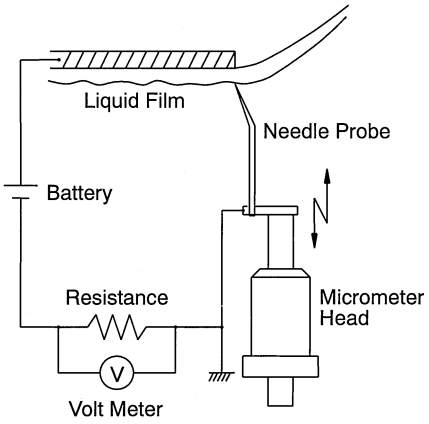

Fig. 4 Principle of contact needle method.

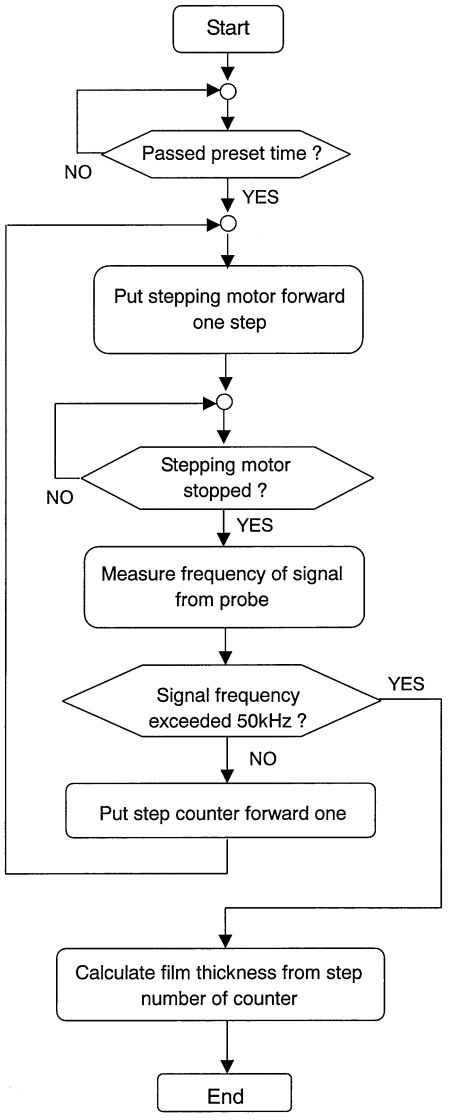

Fig. 6 Flowchart of film thickness measurement.

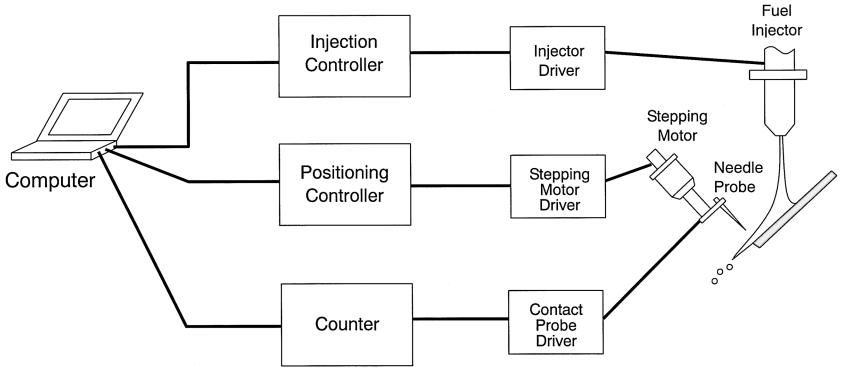

Fig. 5 Measurement system of liquid-film thickness.

Table 1 Physical properties of used liquids at 293 K

Liquid	Density, kg/m^3	Viscosity, mPa s	Surface tension, mN/m
Tap water	998	1.002	72.8
Dry solvent	775	0.792	24.5

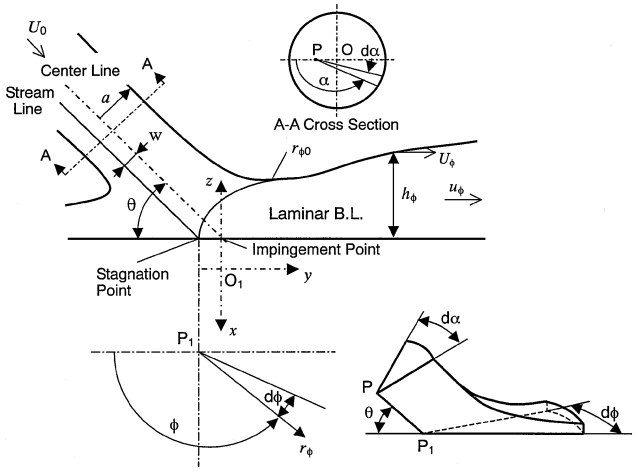

Fig. 7 Symbols and coordinate system employed in theoretical analysis of liquid-film flow.

conductivity. Dry solvent (Nippon Mitsubishi Oil Co.) was used in the spray characteristics measurement because it is safe and has similar properties to fuel. The liquid injection pressures ranged from 6 to 15 MPa.

Theoretical Analysis

Liquid-Film Flow on Solid Wall

In the case of the oblique impingement of the liquid jet onto the solid wall, the liquid-film flow on the solid wall was theoretically analyzed. Prior to this analysis, the following assumptions were made:

1) The liquid flow is two-dimensional.

2) The velocity distribution across the liquid jet is uniform, and the liquid flows inside the liquid jet and the liquid film on the solid wall are laminar.

3) On the solid wall, the laminar boundary layer develops in the liquid film from the stagnation point.

4) The velocity distribution across a laminar boundary layer can be approximated by the following quartic equation of Ishigai et al.[19]:

$$u = U(2\eta - 2\eta^3 + \eta^4) \tag{1}$$

5) The liquid flowing in a minute angle $d\alpha$ in the liquid jet flows in a minute angle $d\phi$ in the liquid film as shown in Fig. 7, where the following geometric relationship of Rubel[20] exists between α, ϕ, and θ;

$$\tan\phi = \sin\theta \cdot \tan\alpha \tag{2}$$

6) In the case of the oblique impingement of a liquid jet on the solid wall, the centerline of a jet is not consistent with a streamline passing the stagnation point on the wall as shown in Fig. 7. The space between these two lines is expressed by the following equation[21]:

$$w = a\cos\theta \tag{3}$$

7) The effect of the airflow on the liquid film and that of the gravity on the film behavior can be ignored.

In the actual liquid-film flow on a solid wall, the hydraulic jump takes place at the periphery, and then the film thickness increases rapidly. The conditions present when the hydraulic jump takes place are greatly affected by the roughness and inclination of the wall surface, operating conditions, etc. On the other hand, the flow rate of a liquid passing through a thick rim generated at the periphery as a result of the hydraulic jump is estimated to be small compared to the total liquid flow rate. So, the effect of the hydraulic jump on the spray characteristics seems to be small. Thus, in the present theoretical analysis the hydraulic jump was not taken into account for simplification. However, at the design of the actual fuel injector it should be considered that the thick rim generated at the periphery by the hydraulic jump can result in a deposition. The effect of the hydraulic jump on an injector performance is left to future study.

The symbols and the coordinate system used in the theoretical analysis are shown in Fig. 7. As aforementioned, in the case of oblique impingement at the intersection point O_1 between the centerline of a jet and the solid wall disagrees with the stagnation point P_1.

The momentum equation of a laminar boundary layer is expressed generally by the following equation using the cylindrical coordinate[22]:

$$\left(\frac{\mathrm{d}}{\mathrm{d}r} + \frac{1}{r}\right)\int_0^\delta u(U_0 - u)\,\mathrm{d}z = \nu_l\left(\frac{\partial u}{\partial z}\right)_{z=0} \tag{4}$$

The film flow is classified using the point ($r_\phi = r_{\phi 0}$), where the laminar boundary layer reaches the film surface:

1) In the case that $r_\phi \le r_{\phi 0}$, the velocity distribution across the laminar boundary layer is expressed by the following equation:

$$u_\phi = U_0\left(2\eta_1 - 2\eta_1^3 + \eta_1^4\right) \tag{1'}$$

where $\eta_1 = z/\delta_\phi$.

By the substitution of Eq. (1′) for Eq. (4), one deduces the following equation:

$$\delta_\phi^* = 5.97\sqrt{r_\phi^*} \tag{5}$$

where

$$r_\phi^* = (r_\phi/a)\cdot 1/Re^{\frac{1}{3}} \tag{6}$$

$$\delta_\phi^* = (\delta_\phi/a)\cdot Re^{\frac{1}{3}} \tag{7}$$

$$Re = Q/(a\,\nu_l) \tag{8}$$

The continuity condition at $r_\phi = r_{\phi 0}$ and assumption (5) allow one to deduce the following equation:

$$r_{\phi 0}^* = \left[0.564/(4\pi)^{\frac{1}{3}}\right] A^{\frac{2}{3}} B^{\frac{4}{3}} \tag{9}$$

where

$$A = \frac{\sin\theta}{\sin^2\phi + \cos^2\phi\cdot\sin^2\theta} \tag{10}$$

$$B = \pm\varepsilon\sqrt{\frac{\sin^2\theta}{\tan^2\phi + \sin^2\theta}} + \sqrt{1 - \frac{\varepsilon^2\tan^2\phi}{\tan^2\phi + \sin^2\theta}} \tag{11}$$

where a sign of the first term in the right side of Eq. (11) is negative when $0 \le \alpha < 90$ deg and positive when $90 \le \alpha < 180$ deg.

The continuity equation produces the following equation of the film thickness:

$$h_\phi^* = 1\Big/\left(2r_\phi^*\right)A\cdot B^2 + 1.79\sqrt{r_\phi^*} \tag{12}$$

where

$$h_\phi^* = (h_\phi/a)Re^{\frac{1}{3}} \tag{13}$$

2) In the case that $r_\phi > r_{\phi 0}$, the velocity distribution across the laminar boundary layer is expressed by the following equation:

$$u_\phi = U_\phi\left(2\eta_2 - 2\eta_2^3 + \eta_2^4\right) \tag{1''}$$

where $\eta_2 = z/h_\phi$.

The substitution of Eq. (1″) for Eq. (4), the continuity condition at $r_\phi = r_{\phi 0}$, and assumption (5) produce the following equation:

$$h_\phi^* = \frac{0.642}{r_\phi^*} A \cdot B^2 + \frac{5.03 r_\phi^{*2}}{A \cdot B^2} \tag{14}$$

The velocity of the liquid-film surface is expressed by the following equation:

$$U_\phi / U_0 = 1 \Big/ \left(0.899 + 7.04 A^{-2} B^{-4} r_\phi^{*3}\right) \tag{15}$$

Mean Droplet Size of Spray Issued from Wall Impingement Injector

Dombrowski and Johns[11] and Fraser et al.[12] deduced a liquid-film breakup model. They hypothesized that the liquid film disintegrates every half-wavelength of a sinuous wave. A fraction generated by the disintegration of the liquid film becomes a liquid stem as a result of the surface tension. A liquid stem disintegrates into a droplet every one wavelength. In this paper, the mean droplet size of the spray issued from the wall impingement injector was predicted according to the model by Dombrowski and Johns.[11] The velocity distribution across a liquid film issuing from the wall edge becomes uniform rapidly, and the liquid film seems to disintegrate by the same breakup mechanism as a free liquid film issuing from a fan spray nozzle. Therefore, it was assumed as a first-order approximation that a liquid film spreads radially from the stagnation point as a free liquid film. The velocity distribution across the free liquid film was assumed to be uniform. The liquid velocity remains constant along the streamline in the free liquid film, and it is equal to the mean film velocity at the wall edge calculated by using Eqs. (1″) and (15).

Dombrowski and Johns[11] deduced the following equation about the mean droplet size employing the Squire's theory for liquid film disintegration[9] and Weber's theory for liquid stem disintegration[23]:

$$d_m = 1.882 \cdot d_L [1 + 3Oh_l]^{\frac{1}{6}} \tag{16}$$

where the diameter of the liquid stem d_L is expressed by the following equation:

$$d_L = 0.9614 \left[\frac{K^2\sigma^2}{\rho_a \rho_l U_e^4}\right]^{\frac{1}{6}} \left[1 + 2.60\mu_l \left(\frac{K\rho_a^4 U_e^7}{72\rho_l^2\sigma^5}\right)^{\frac{1}{3}}\right]^{\frac{1}{5}} \tag{17}$$

The Oh_l and K in Eqs. (16) and (17), respectively, are expressed by the following equations:

$$K = L \cdot h_e \tag{18}$$

$$Oh_l = \mu_l \Big/ \sqrt{\rho_l \sigma d_L} \tag{19}$$

The U_e and h_e in Eqs. (17) and (18), respectively, are calculated using Eqs. (13–15). The distance from the stagnation point to the solid wall edge L of the injector used in the measurement of the spray characteristics is equal to 3.29 mm.

Dombrowski and Johns[11] proposed the following semi-empirical equation about the Sauter mean diameter by comparing the measurements:

$$d_{32} = 1.186 \cdot d_L [1 + 3Oh_l]^{\frac{1}{6}} \tag{20}$$

In this paper, the following equation is proposed about the Sauter mean diameter:

$$d_{32} = 0.6 \cdot d_L [1 + 3Oh_l]^{\frac{1}{6}} \tag{21}$$

The initial thickness and initial velocity of the free liquid film were determined from the calculated film thickness and velocity distribution of the liquid film at the wall edge by theoretical analysis of the film flow, assuming mass and momentum conservation of liquid at the wall edge.

The correlation factor on the right-hand side of Eq. (21) was determined by comparing the mean diameter with the measurements. The correlation factor in Eq. (21) is about half of Eq. (20) proposed by Dombrowski and Johns.[11] In the present case, the relative velocity between the liquid film and the surrounding air is larger than the case of Dombrowski and Johns. Thus, the ratio of finer spray droplets generated from the waves on the film surface by the Kelvin–Helmholtz instability to the total spray droplets becomes larger than in the case of Dombrowski and Johns. These droplets reduce the Sauter mean diameter. However, because the spray formation mechanism proposed by Dombrowski and Johns still remains, the effects of the injection conditions and the physical properties of air and liquid on the mean diameter in the present case are qualitatively the same as in the case of Dombrowski and Johns. In the present model of film breakup, the film flow on the solid wall was neglected. The effect of this simplification on the mean diameter cannot be estimated at the present state. The correlation factor of Eq. (21) seems to include these effects.

Comparisons Between Analysis and Measurement and Discussions

Liquid-Film Thickness

The liquid-film thicknesses were measured by the newly developed automatic film thickness measurement system and then were compared to the theoretical analysis. At first, to verify the measurement accuracy of the system the film thickness measurements were carried out using nozzle 1 shown in Fig. 2a. Figures 8 and 9 show the measurements from the automatic measurement system compared with the theoretical analysis and the measurements from the manually operated system using the micrometer head to position the needle probe. Figure 8 shows the measurements in the case of normal impingement, and Fig. 9 is in the case of oblique impingement. The measurements from the automatic measurement system are almost coincidental to the measurements from the manually operated system as well as the theoretical analysis except far from the center.

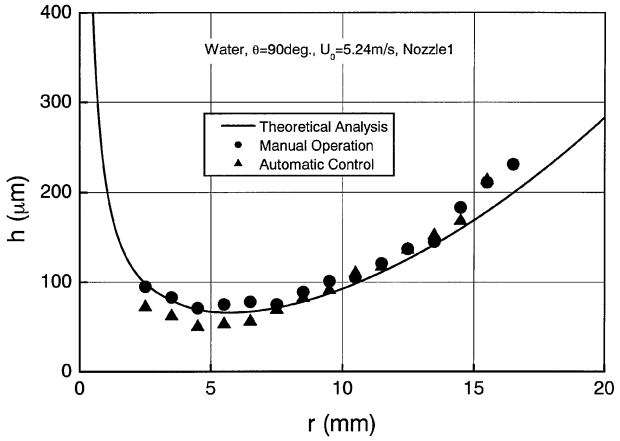

Fig. 8 Comparisons of film thickness using large diameter nozzle (in the case of normal impingement).

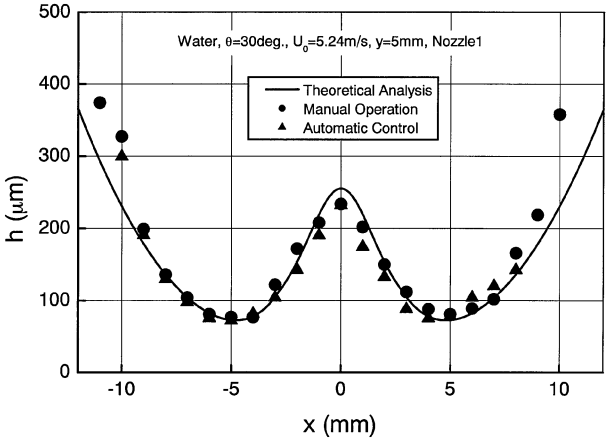

Fig. 9 Comparisons of film thickness using large diameter nozzle (in the case of oblique impingement).

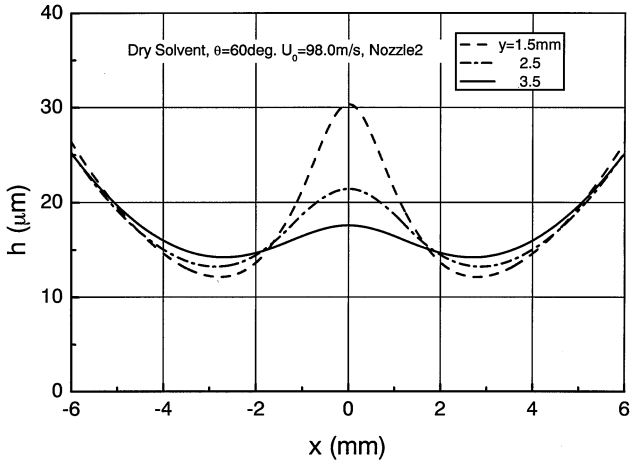

Fig. 10 Calculations of film thickness distribution against distance from impingement point.

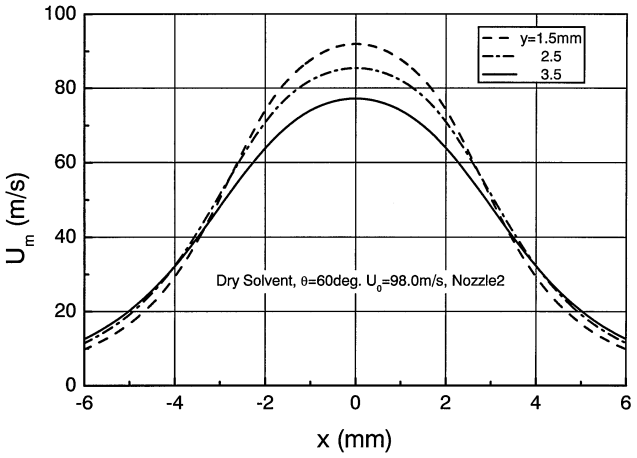

Fig. 11 Calculations of mean film velocity distribution against distance from impingement point.

The discrepancies of the measurements from the theoretical analysis at the periphery of the liquid film are caused by the effects of the hydraulic jump on the film thickness. In the theoretical analysis, the effects of the hydraulic jump on the film flow were not taken into consideration.

Figures 10 and 11 show the results of the theoretical analysis of the film thickness distribution and mean velocity distribution of a dry solvent film at several distances from the impingement point, respectively. These numerical results were calculated under the condition that the liquid impingement angle was $\theta = 60$ deg and the liquid impingement velocity was $U_0 = 98.0$ m/s. The following calculations were carried out using nozzle 2 shown in Fig. 2b. As the distance from the centerline x increases, the film thickness decreases at first and then increases. The film thickness has a minimum value at approximately 3 mm far from the centerline for all y values. As the distance from the impingement point y increases, the film thickness distribution becomes flat, and the peak at $x = 0$ decreases rapidly. The mean velocity of the liquid film decreases monotonously as x increases. The peak of the mean velocity at $x = 0$ is close to the liquid impingement velocity. The effect of distance y on the mean velocity distribution near the centerline is smaller than that on the film thickness distribution.

Figures 12–14 show the measurements of film thicknesses compared with the results of the theoretical analysis. The measurements shown in these figures were carried out varying distance y under liquid injection pressure $P_i = 8$ MPa. In the calculations of the film thickness, the liquid impingement velocity U_0 was calculated from the liquid flow rate and the measurements of the liquid jet diameter just before the impingement. The velocity distribution in the liquid

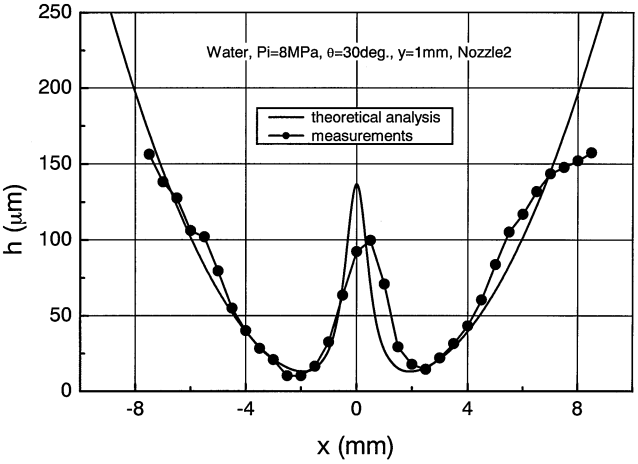

Fig. 12 Comparison of film thickness (in the case of $y = 1$ mm).

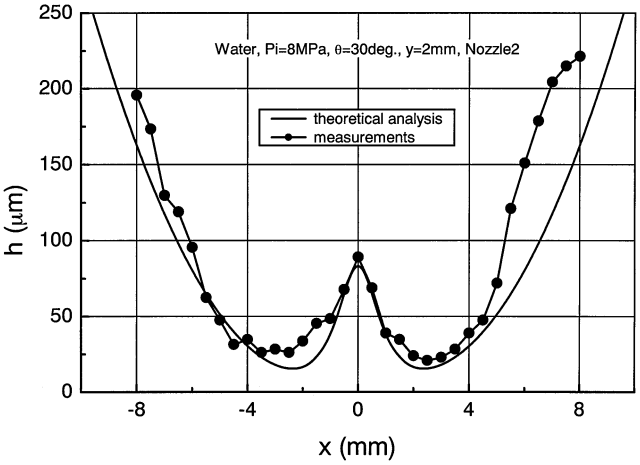

Fig. 13 Comparison of film thickness (in the case of $y = 2$ mm).

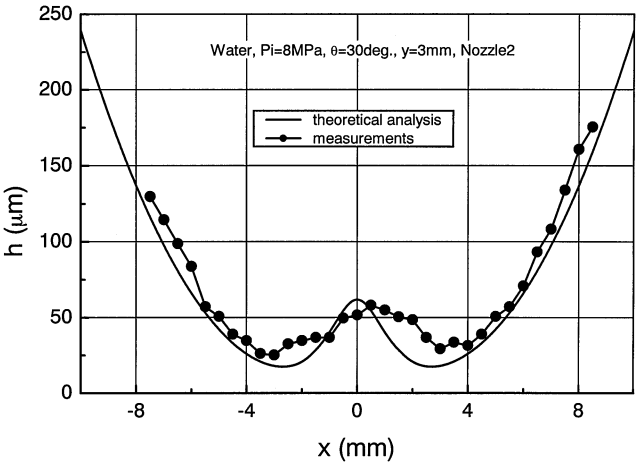

Fig. 14 Comparison of film thickness (in the case of $y = 3$ mm).

jet was assumed to be uniform (see assumption of theoretical analysis). The measured liquid jet diameter just before the impingement equals 0.46 mm for both liquids and for every injection pressure from 6 to 12 MPa. Table 2 shows the calculated liquid impingement velocity against the liquid injection pressure used in the film thickness calculations for both liquids.

In the figures, the film thickness decreases rapidly at first, with a minimum value around at $x = 2$ mm, and then increases. This trend is consistent qualitatively in both calculations and measurements. The calculations are almost coincidental quantitatively with

Table 2 Impingement velocity used in film thickness calculations

P_i, MPa	U_0, m/s
6	44.5
7	47.5
8	50.5
9	53.5
10	56.5
11	59.4
12	62.4

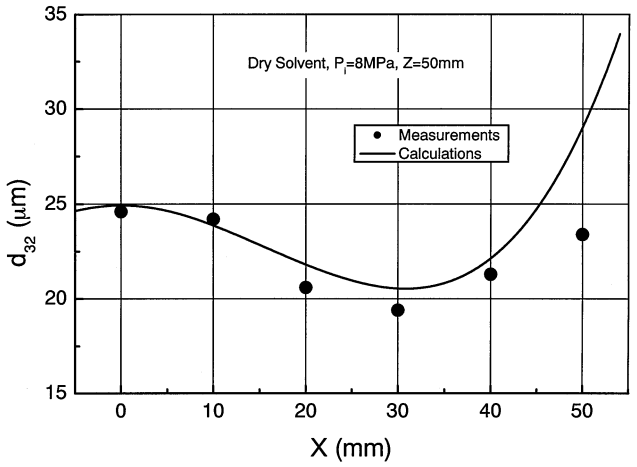

Fig. 15 Comparison of mean droplet diameter distribution (in the case of $P_i = 8$ MPa).

the measurements. In Fig. 13, the discrepancies of the film thickness are observed at the periphery. These discrepancies are caused by the hydraulic jump, as aforementioned. In Fig. 14, the measurements show larger thicknesses than the calculations at the position where the film thickness becomes a minimum. The discrepancies of the minimum film thickness downstream (at $y = 3$ mm) seem to be caused by the measurement method. In the present case, the disturbance waves with high frequency exist on the liquid film surface. These waves are caused by the turbulence of a liquid flow in the nozzle. Because the wavelength of a disturbance wave on the film surface is quite small compared to the large wave that gives rise to the liquid film breakup, the contribution of a disturbance wave with high frequency on the breakup seems to be small. The disturbance wave is amplified downstream, and the liquid makes contact with the tip of the needle probe intermittently. In the case of a high-frequency wave, the peak of the wave makes contact with the needle probe before the front trough is detached from it. Thus, the contact needle probe overcalculates the film thickness. These errors will take place when the waves with large amplitude and high frequency exist on the liquid surface.

Sauter Mean Diameter

The measurements of the Sauter mean diameter reported in a previous paper[1] were used for the comparisons of the calculations.

Figures 15 and 16 show the Sauter mean diameter distributions compared with the calculations. The liquid injection pressure is 8 MPa in Fig. 15 and 12 MPa in Fig. 16. As the distance from the centerline X increases, the mean diameter decreases, and it has a minimum value of approximately $X = 30$ mm. Then it increases in either case. This qualitative trend of the mean diameter is consistent in both calculations and measurements and coincides with that of the liquid-film thickness shown in Figs. 12–14.

Figure 17 shows the effect of the injection pressure on the Sauter mean diameter compared with the calculations. The measurements were carried out at the center of the spray sheet, that is, $X = 0$. The mean diameter decreases monotonously as the injection pressure increases. As the injection pressure increases, the film thickness

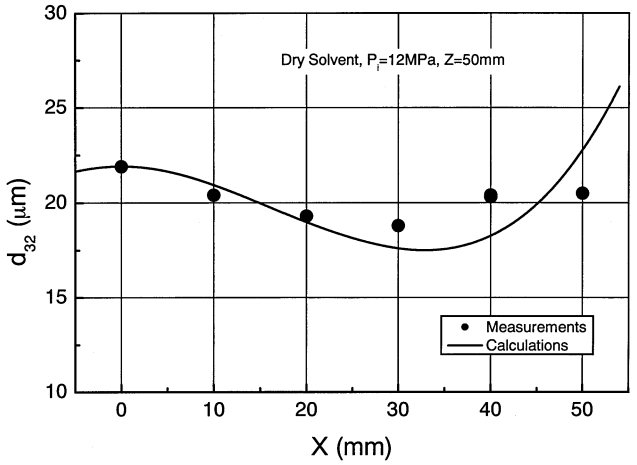

Fig. 16 Comparison of mean droplet diameter distribution (in the case of $P_i = 12$ MPa).

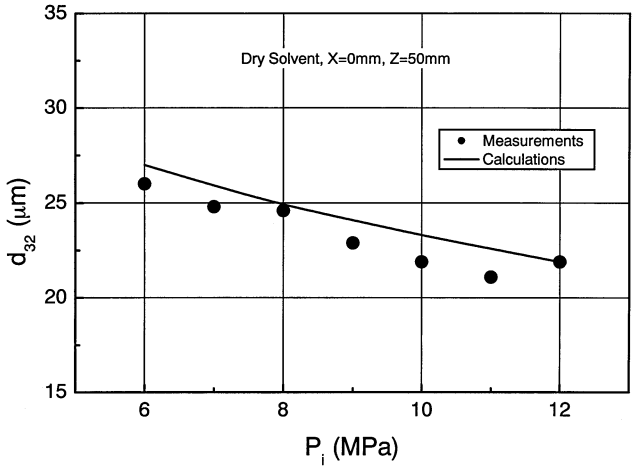

Fig. 17 Effect of liquid injection pressure on mean droplet diameter.

decreases, and the relative velocity between the liquid film and the surrounding air increases. Thus, the droplet size decreases. The calculations of the mean droplet size agree well with the measurements.

Conclusions

The liquid-film flow on the wall generated by the impingement of the liquid jet onto the solid wall was investigated theoretically and experimentally. The film flow on the wall was analyzed theoretically using the laminar boundary-layer model. The film thicknesses on the wall were measured by the newly developed automatic film thickness measurement system. In spite of several assumptions that were made in the theoretical analysis, the calculations of the film thickness by the theoretical analysis yielded comparable values to the measurements except at the periphery of the liquid film. At the periphery, the film thickness increases rapidly because of the hydraulic jump. On the other hand, a hydraulic jump was not taken into consideration in the theory because of the difficulty in obtaining an estimate of the conditions on which a hydraulic jump occurs. This simplification in the theoretical analysis resulted in the discrepancies of the film thickness at the periphery. The mean droplet sizes of the spray injected from the newly developed wall impingement injector were predicted by using the liquid film breakup model proposed by Dombrowski and Johns[11] and the present theoretical analysis of the film flow on the wall. The correction factor in the prediction equation of the mean droplet size was determined by the comparisons of the measurements. The mean droplet size decreased at first, and then increased after it reached the minimum value, as the measurement point moved toward the periphery from the center of the spray sheet. This trend was consistent qualitatively with that of the film thickness

along the line that was perpendicular to the liquid injection direction. The predictions of the mean droplet size showed good agreement with the measurements.

Acknowledgments

The authors express their thanks to Y. Ogawa of Toyota Motor Co., T. Saito of Hirosaki University, and S. Tanno of Tohoku University for their help with the experiments.

References

[1]Inamura, T., and Tomoda, T., "Characteristics of Sprays Through a Wall Impingement Injector," *Atomization and Sprays* (to be published).

[2]Gosman, A. D., and Ioannides, E., "Aspects of Computer Simulation of Liquid-Fueled Combustors," *Journal of Energy*, Vol. 7, No. 6, 1983, pp. 482–490.

[3]Faeth, G. M., "Mixing, Transport and Combustion in Sprays," *Progress in Energy and Combustion Science*, Vol. 13, 1987, pp. 293–345.

[4]Reitz, R. D., "Modeling Atomization Processes in High-Pressure Vaporizing Sprays," *Atomisation and Spray Technology*, Vol. 3, No. 4, 1987, pp. 309–337.

[5]O'Rourke, P. J., and Amsden, A. A., "The TAB Method for Numerical Calculation of Spray Droplet Breakup," Society of Automotive Engineers, Paper 872089, 1987.

[6]Faeth, G. M., "Structure and Atomization Properties of Dense Turbulent Sprays," *Twenty-Third Symposium (International) on Combustion*, Combustion Inst., 1990, pp. 1345–1352.

[7]Giridharan, M. G., Lee, J. G., Krishnan, A., Przekwas, A. J., and Gross, K., "A Numerical Model for Coupling between Atomization and Spray Dynamics in Liquid Rocket Thrust Chambers," AIAA Paper 92-3768, July 1992.

[8]York, J. L., Stubbs, H. E., and Tek, M. R., "The Mechanism of Disintegration of Liquid Sheets," *Transactions of the ASME*, Vol. 75, 1953, pp. 1279–1286.

[9]Squire, H. B., "Investigation of the Instability of a Moving Liquid Film," *British Journal of Applied Physics*, Vol. 4, 1953, pp. 167–169.

[10]Hagerty, W. W., and Shea, J. F., "A Study of the Stability of Plane Fluid Sheets," *Journal of Applied Mechanics*, Vol. 22, 1955, pp. 509–515.

[11]Dombrowski, N., and Johns, W. R., "The Aerodynamic Instability and Disintegration of Viscous Liquid Sheets," *Chemical Engineering Sciences*, Vol. 18, 1963, pp. 203–214.

[12]Fraser, R. P., Eisenklam, P., Dombrowski, N., and Hasson, D., "Drop Formation from Rapidly Moving Liquid Sheets," *AIChE Journal*, Vol. 8, No. 5, 1962, pp. 672–680.

[13]Miyamoto, T., Kobayashi, T., and Matsumoto, Y., "Structure of Sprays from an Air-Assist Hollow-Cone Injector," Society of Automotive Engineers, Paper 960771, Feb. 1996.

[14]Han, Z., Parrish, S., Farrell, P. V., and Reitz, R. D., "Modeling Atomization Process of Pressure-Swirl Hollow-Cone Fuel Sprays," *Atomization and Sprays*, Vol. 7, No. 6, 1997, pp. 663–684.

[15]Nagaoka, M., and Kawamura, K., "A Deforming Droplet Model for Fuel Spray in Direct-Injection Gasoline Engines," Society of Automotive Engineers, Paper 2001-01-1225, March 2001.

[16]Dombrowski, N., Hasson, D., and Ward, D. E., "Some Aspects of Liquid Flow Through Fan Spray Nozzle," *Chemical Engineering Sciences*, Vol. 12, 1960, pp. 35–50.

[17]Dombrowski, N., and Hooper, P. C., "The Effect of Ambient Density on Drop Formation in Sprays," *Chemical Engineering Sciences*, Vol. 17, 1962, pp. 291–305.

[18]Azuma, T., and Hoshino, T., "The Radial Flow of a Thin Liquid Film (2nd Report)," *Transactions of the Japan Society of Mechanical Engineers (Ser. B)*, Vol. 50, No. 452, 1984, pp. 982–989 (in Japanese).

[19]Ishigai, K., Nakanishi, S., Mizuno, M., and Imamura, T., "Heat Transfer by Impingement of Round Water Jet," *Transactions of the Japan Society of Mechanical Engineers (Ser. 2)*, Vol. 42, No. 357, 1976, pp. 1502–1510 (in Japanese).

[20]Rubel, A., "Computations of the Oblique Impingement of Round Jets upon a Plane Wall," *AIAA Journal*, Vol. 19, No. 7, 1981, pp. 863–871.

[21]Hasson, D., and Peck, R. E., "Thickness Distribution in a Sheet Formed by Impinging Jets," *AIChE Journal*, Vol. 10, No. 5, 1964, pp. 752–754.

[22]Watson, E. J., "The Radial Spread of a Liquid Jet over a Horizontal Plate," *Journal of Fluid Mechanics*, Vol. 20, No. 3, 1964, pp. 481–499.

[23]Weber, C., "Zum Zerfall eines Flussigkeitsstrahles," *Zeitschrift für Angewandte Mathematik und Mechanik,* Vol. 11, No. 2, 1931, pp. 136–154.

S. K. Aggarwal
Associate Editor